Translational and rotational diffusion of a single nanorod in unentangled polymer melts

Min Jung Kim,[1] Hyun Woo Cho,[1] Jeongmin Kim,[1] Heesuk Kim,[2] and Bong June Sung[1,*]
[1]*Department of Chemistry and Research Institute for Basic Science, Sogang University, Seoul 121-742, Republic of Korea*
[2]*Photo-electronic Hybrids Research Center, Korea Institute of Science and Technology (KIST), Seoul 136-791, South Korea*
(Received 22 January 2015; revised manuscript received 16 September 2015; published 7 October 2015)

Polymer nanocomposites have been an issue of both academic and industrial interest due to promising electrical, mechanical, optical, and magnetic properties. The dynamics of nanoparticles in polymer nanocomposites is a key to understanding those properties of polymer nanocomposites and is important for applications such as self-healing nanocomposites. In this article we investigate the translational and the rotational dynamics of a single nanorod in unentangled polymer melts by employing extensive molecular dynamics simulations. A nanorod and polymers are modeled as semiflexible tangent chains of spherical beads. The stiffness of a nanorod is tuned by changing the bending potential between chemical bonds. When polymers are sufficiently long and the nanorod is stiff, the nanorod translates in an anisotropic fashion along the nanorod axis within time scales of translational relaxation times even in unentangled polymer melts. The rotational diffusion is suppressed more significantly than the translational diffusion as the polymer chain length is increased, thus the translational and rotational diffusion of the nanorod are decoupled. We also estimate the winding numbers of polymers, i.e., how many times a polymer winds the nanorod. The winding number increases with longer polymers but is relatively insensitive to the nanorod stiffness.

DOI: 10.1103/PhysRevE.92.042601 PACS number(s): 36.20.Ey, 81.05.Qk, 83.80.Ab

I. INTRODUCTION

Polymer nanocomposites, mixtures of nanoparticles and polymers, have drawn attention because one can design novel materials with desirable properties of both polymers and nanoparticles [1–6]. For example, one may prepare isotropic conductive adhesives by mixing conductive silver nanowires and epoxy [7]. The major stumbling block to developing novel polymer nanocomposites is the poor dispersion of nanoparticles in polymer matrices [8,9]. In order to enhance the dispersion, therefore, the intermolecular interaction between nanoparticles and polymers has been studied extensively by either modifying the surface of nanoparticles or introducing dispersing agents [10–12]. Recent studies showed that the diffusion of nanoparticles in polymer matrices should relate closely to the dispersion kinetics of nanoparticles [13]. The dynamics of nanoparticles in polymer melts, however, has drawn relatively less attention. The translational and rotational diffusion of nanoparticles is also critical to the development of self-healing materials [14] and provides rheological information [15] on various length scales [16–18]. In this work, we perform molecular dynamics simulations in order to investigate the translational and rotational diffusion of a single nanoparticle, especially a nanorod, in unentangled polymer melts.

Stokes-Einstein (SE) and Stokes-Einstein-Debye (SED) relations describe the translational and rotational diffusion of nanoparticles, respectively, in polymers above the glass transition temperature (T_g) [19]. Both relations suggest that the translational diffusion coefficient (D_T) and the rotational diffusion coefficient (D_R) of nanoparticles should be proportional to T/η, where T and η are temperature and polymer viscosity, respectively. There have been, however, reports that the SE relation breaks down depending on either T or the size of nanoparticles [20]. For example, D_T of cadmium selenide nanoparticles was about 200 times faster than predicted by the SE relation when the nanoparticle size was smaller than the entanglement mesh [21]. Other experiments illustrated that, as T approached T_g, D_T and D_R showed different temperature dependencies. Recent theoretical and simulation studies illustrated systematically that the diffusion of nanoparticles should be determined by the nanoparticle size (R), the polymer size, the polymer correlation length (ξ), and polymer entanglements [22–24]. In our simulations we also find that the rotational diffusion of a single nanorod is suppressed more than the translational diffusion as the degree of polymerization of polymer melts increases.

In case of a nonspherical nanoparticle such as a nanorod, sufficiently long polymers may wrap the nanorod, and the rotational and translational dynamics of the nanorod would become complicated [25–30]. When the aspect ratio of nanorods is sufficiently large, both the translational and rotational dynamics would decrease significantly [31]. A recent simulation study showed that, as the aspect ratio increased from 5 to 10, both D_T and D_R decreased by a factor of 30, which affected the dispersion and aggregation kinetics significantly. In the meantime, recent single molecule fluorescence imaging experiments illustrated that in entangled F-actin filaments, actin filaments (nonspherical particles) underwent an anisotropic translational diffusion [32]. A rodlike virus in the nematic phase also showed an anisotropic diffusion with a much larger diffusion coefficient along the nematic director [33]. Even in isotropic solutions, the translational diffusion of nanorods showed anisotropic behaviors if the nanorod concentration increased up to semidilute solutions [34]. In this study we find that, even in isotropic unentangled polymer melts, the translational diffusion is anisotropic within the translational relaxation time. Such an anisotropic translational motion disappears after the rotational relaxation time.

The diffusion of polymers in polymer nanocomposites also plays critical roles in various applications and has been studied extensively. Recent systematic studies revealed that there

*Corresponding author: bjsung@sogang.ac.kr

should exist a universal scaling relation for polymer diffusion in nanocomposites in the case of spherical nanoparticles and that the nanoparticle size, interparticle spacing, and polymer size should play critical roles in polymer diffusion [35–40]. When carbon nanotubes (CNTs) were introduced to polymers, the polymer diffusion showed a nonmonotonic behavior as a function of the CNT concentration [41,42]. The addition of carbon nanotubes decreased the polymer diffusion initially, but the polymer diffusion coefficient increased beyond a critical carbon nanotube concentration. It was revealed that the polymer diffusion should be determined by the intermolecular interaction, polymer entanglement, and carbon nanotube size [43,44].

In this paper, we employ molecular dynamics simulations to investigate the translational and rotational dynamics of a single nanorod in unentangled polymer melts. When polymers are sufficiently long, D_T and D_R depend on the polymer chain length (or viscosity) in different fashions. It is interesting that the translational diffusion of the nanorod becomes anisotropic even in unentangled polymers at the time scales of the translational relaxation time. Such an anisotropic diffusion is most pronounced for the longest and stiffest nanorod in relatively long polymer melts. We estimate the winding number (W) of a polymer around a bead of the nanorod, i.e., how much the polymer wraps the nanorod [45]. The winding number (W) increases with an increase in the degree of polymerization (N) of polymers. But W is relatively insensitive to the flexibility of the nanorod. We also estimate the total winding number (T, the sum of W's for all neighbor polymers) and the effective winding number (S, the sum of W's for $W \geqslant 0.5$) in order to study how several polymers may wind and influence the nanorod simultaneously.

The rest of the paper is organized as follows. The simulation model and methods are described in Sec. II, results are presented and discussed in Sec. III, and a summary and conclusions are presented in Sec. IV.

II. MODEL AND SIMULATION METHODS

Metal-based nanorods would be quite rigid while CNTs would be more flexible. One can even tune the stiffness and the length of CNTs either by modifying their surface or by undergoing sonication. The various physical properties such as the modulus of composites depend on the stiffness of CNTs because the stiffness might influence the way a polymer and a CNT would interact with each other. In order to investigate nanorods of different stiffness, we model the nanorod as a semiflexible chain of $N_{\rm rod}(=20)$ spheres of diameter σ, which is the unit of length in this study. Two neighbor spheres of the nanorod are bonded by employing a harmonic potential $U_h = K_h(r - r_0)^2$, where r is the distance between two spheres. In this study $K_h = 500 k_B T \sigma^{-2}$ and $r_0 = 1.3\sigma$, where k_B and T denote the Boltzmann constant and temperature, respectively. $k_B T$ is the energy unit of this study, i.e., $k_B T = 1$. Between two consecutive chemical bonds of the nanorod is a bending potential $U_b = K_b(\theta - \theta_0)^2$, where θ is the angle between two chemical bonds, $\theta_0 = \pi$ and K_b ranges from 0 to 20. K_b is a parameter to control the stiffness of the nanorod. The nonbonding interaction between spheres of the nanorod is described using the Weeks-Chandler-Adersen (WCA) potential (U_{nb}) as follows:

$$U_{nb}(r) = \begin{cases} 4\epsilon\left[\left(\frac{\sigma}{r}\right)^{12} - \left(\frac{\sigma}{r}\right)^{6}\right] + \epsilon, & r \leqslant 2^{1/6}\sigma, \\ 0, & r > 2^{1/6}\sigma, \end{cases}$$

where $\epsilon = k_B T$ [45].

Polymers are modeled as semiflexible chains of monomers, too. But we employ the finitely extensible non-linear elastic (FENE) potential (U_F) to describe the chemical bonds of monomers, i.e.,

$$U_F(r) = -0.5 K_f R_0^2 \ln\left[1 - \left(\frac{r}{R_0}\right)^2\right] + 4\epsilon\left[\left(\frac{\sigma}{r}\right)^{12} - \left(\frac{\sigma}{r}\right)^{6}\right] + \epsilon, \quad (1)$$

where $R_0 = 1.5$ and $K_f = 30$. The nonbonding interaction between monomers of polymers is also described by the same WCA potential (U_{nb}). However, the interaction between a monomer and a sphere of the nanorod is described by a truncated and shifted Lennard-Jones potential with a cutoff distance of 2.5σ and a well depth of $k_B T$. Our model is quite similar to previous computational studies [46] in various aspects: (1) both polymers and a nanorod are modeled as bead-spring models, (2) the diameter of beads for a nanorod is identical to that of monomers, and (3) the harmonic bonding potential is used to describe the nanorod. Such a model for nanorod-polymer composites may correspond to the polymer nanocomposites of either short CNTs or nanowires. In some experiments the size of nanorods is comparable to or smaller than the polymer size, which is consistent with our model [41,42]. Our system temperature of $T = 1$ is well above the glass transition temperature because both polymers and the nanorod are diffusive in our simulation times.

Initial configurations of a single nanorod and polymers are obtained by placing the nanorod in a cubic simulation cell of dimension $L = 50\sigma$. Then, polymers are inserted at random positions. If a newly inserted polymer, placed at a random position, overlaps with preexisting molecules, i.e., the shortest distance between beads of the polymer and preexisting molecules is smaller than σ, the random position is discarded and a new random position is tried. This procedure is repeated until the number density of polymer ($\rho = N N_p / L^3$) is 0.8. N and N_p are the degree of polymerization and the number of polymers in the simulation cell, respectively. In our study, N and N_p range from 1 to 64 and from 100 000 to 1562, respectively. It was reported that in the case of polymer melts with FENE chemical bond potential and Lennard-Jones nonbonding interaction potential, the entanglement length (N_e) is about 85. Because $N < N_e$ in our study, we expect that the entanglements of polymers hardly occur in our systems [47]. Initial configurations are equilibrated in the canonical ensemble by performing molecular dynamics simulations until both the nanorod and polymers diffuse translationally more than their own size; i.e., the mean-square displacements [$\langle(\Delta r)^2(t)\rangle$] of molecules are larger than the radius of gyration R_g^2 of polymers and the nanorod. We employ the LAMMPS molecular dynamics simulator to perform molecular dynamics simulations. We use a Nosé-Hoover thermostat and the velocity-Verlet integrator with a time step of 0.002.

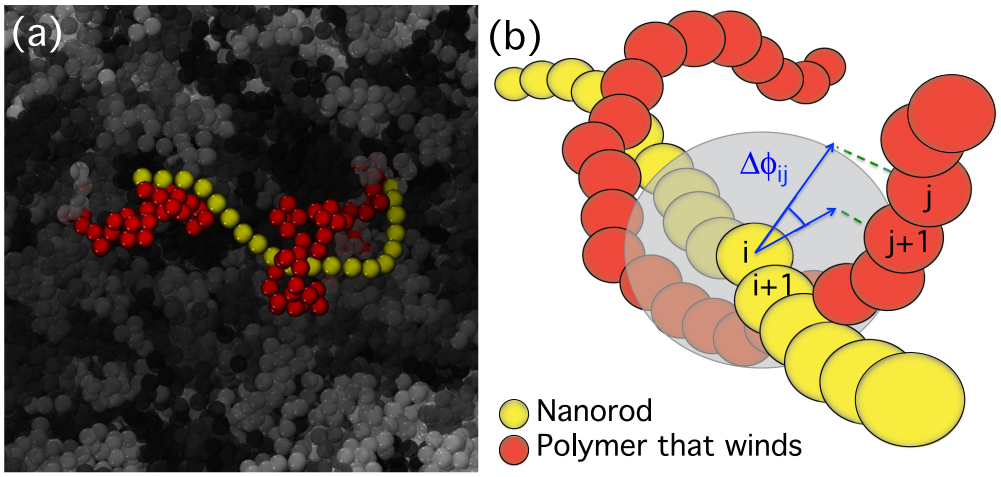

FIG. 1. (Color online) (a) A simulation snapshot for $N = 32$ and $K_b = 20$. A yellow molecule is the nanorod. Red polymers are ones that wind the nanorod with the winding number $W > 0.6$. Grey polymers do not wrap but interact with the nanorod via nonbonding intermolecular interactions. (b) A schematic for the estimation of the winding number W. $\Delta\phi_{ij}$ is the angle between two vectors projected onto the surface perpendicular to the chemical bond of the nanorod.

The number density of the nanorod is 0.8×10^{-5} and is much smaller than that of polymers. Therefore, the presence of a single nanorod in the system does not influence the polymer diffusion, especially the mean-square displacements of polymers. However, if one were to add many nanorods to the polymer matrices, the viscosity would increase in proportion to the intrinsic viscosity of the nanorod, which should affect both the dynamics of nanorods and polymers. In this study, we consider a limiting case of only one nanorod in polymer matrices.

Polymers in our systems are expected to follow Rouse dynamics because polymers are too short to be entangled significantly. We investigate the translational and rotational diffusion of polymers by calculating the mean-square displacement $[\langle(\Delta r)^2(t)\rangle]$ of the centers of mass of polymers and the time correlation functions $[U(t)]$ of the end-to-end vectors of polymers. The translational (τ_{pT}) and rotational (τ_{pR}) relaxation times of polymers are estimated by using the relations $\langle(\Delta r)^2(t = \tau_{pT})\rangle = R_g^2$ of polymers and $U(t = \tau_{pR}) = e^{-1}$, respectively. As expected for the Rouse dynamics, $\tau_{pT} \sim N^2$ and $\tau_{pR} \sim N^2$ for $N \geqslant 32$ (not shown). This suggests that polymers in our simulations should not be entangled significantly.

We quantify how much a polymer winds the nanorod by estimating the winding number W. For a given configuration of the nanorod and polymers, we first find a set of neighbor polymers of which the shortest distance between their monomers and the nanorod is within a distance of 1.5σ. As depicted in Fig. 4(a), neighbor polymers within the distance of 1.5σ form the first shell around the nanorod beads. For each bead i of the nanorod, we obtain vectors ($\mathbf{r}_{ij}$) between the bead and monomers of a neighbor polymer, i.e.,

$$\mathbf{r}_{i,j} = \mathbf{r}_j - \mathbf{r}_i \,, \tag{2}$$

where $\mathbf{r}_j$ and $\mathbf{r}_i$ denote the position vectors of the jth monomer of the neighbor polymer and the ith bead of the nanorod, respectively. We project two vectors $\mathbf{r}_{i,j}$ and $\mathbf{r}_{i,j+1}$ of consecutive monomers of the neighbor polymer onto the plane that is perpendicular to the chemical bond for the ith and the $(i + 1)$th beads of the nanorod [Fig. 1(b)]. Then, the angle $(\Delta\phi_{ij})$ between two projected vectors is obtained. Note that the angle $\Delta\phi_{ij}$ has a different sign depending on the direction of the jth and the $(j + 1)$th monomers' wind. We estimate how much the neighbor polymer winds the nanorod by calculating W as follows:

$$W = \frac{1}{2\pi} \sum_{j=1}^{N-1} \Delta\phi_{ij}. \tag{3}$$

In this study, we estimate values of W only for the ten beads at the center of the nanorod, i.e., $6 \leqslant i \leqslant 15$. Figure 2 depicts six schematic examples of monomers of a polymer that are projected on a plane normal to the chemical bond of a nanorod bead, and corresponding values of W. In case of the last

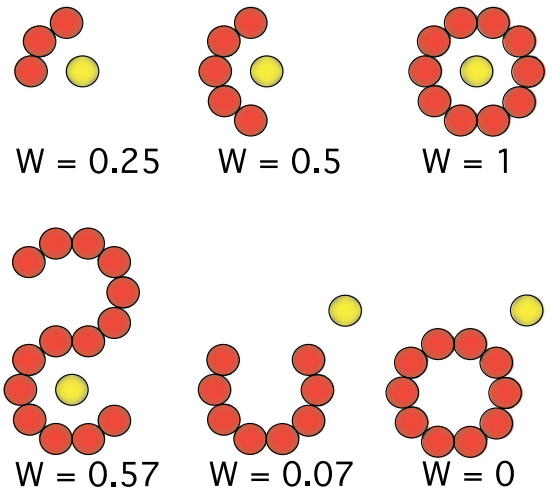

FIG. 2. (Color online) Six schematic examples for how a polymer (red) may wind a nanorod (yellow) and corresponding winding numbers W. Monomers of the polymer and the nanorod bead of interest are projected onto the plane normal to the chemical bond for the nanorod bead.

example with $W = 0$, a polymer makes a circle, outside of which the nanorod is located. In this case, the half of monomers rotate clockwise around the nanorod while other monomers rotate counterclockwise, resulting in $\Delta\phi_{ij}$'s of different signs and $W = 0$.

The total winding number (T) is defined as the sum of all values of W's of neighbor polymers for a given configuration. The effective winding number (S) is obtained by summing the values of W only when $W \geqslant 0.5$. When estimating T, all values of W are summed even though W is small. T may represent how much the nanorod would be wrapped by all neighbor polymers whereas S indicates the degree of effective wrapping with $W \geqslant 0.5$. We obtain the probability distribution functions [$P(W)$, $P(T)$, and $P(S)$] for W, T, and S.

In order to investigate the rotational diffusion of the nanorod, we calculate the time correlation function $U(t) = \langle \mathbf{R}_E(t) \cdot \mathbf{R}_E(0)\rangle / \langle \mathbf{R}_E(0) \cdot \mathbf{R}_E(0)\rangle$, where $\mathbf{R}_E(t)$ $(=\mathbf{r}_1 - \mathbf{r}_{N_{\rm rod}})$ denotes the end-to-end vector of the nanorod at time t [48]. The rotational relaxation time τ_R of the nanorod is estimated by using the relation, $U(t = \tau_R) = e^{-1}$. The translational diffusion of the nanorod is investigated by calculating the mean-square displacement of the center of mass of the nanorod, $\langle (\Delta r)^2(t)\rangle \equiv \langle [\mathbf{r}_c(t) - \mathbf{r}_c(t = 0)]^2\rangle$, where $\mathbf{r}_c(t)$ is the position vector of the center of mass of the nanorod at time t [48]. The translational diffusion coefficient D_T is obtained from $D_T = \lim_{t\to\infty} \langle (\Delta r)^2(t)\rangle / 6t$. We also investigate the anisotropy of the translational diffusion by estimating $\langle (\Delta_\parallel r)^2(t)\rangle$, $\langle (\Delta_\perp r)^2(t)\rangle$, and $A(t)$. $\langle (\Delta_\parallel r)^2(t)\rangle$ and $\langle (\Delta_\parallel r)^2(t)\rangle$ are the mean-square displacements of the nanorod in directions parallel and perpendicular to the end-to-end vector of the nanorod at time $t = 0$, respectively, i.e.,

$$\langle (\Delta_\parallel r)^2(t)\rangle = \left\langle \left(\Delta \mathbf{r}_c(t) \cdot \frac{\mathbf{R_E}(t = 0)}{|\mathbf{R_E}(t = 0)|} \right)^2 \right\rangle, \tag{4}$$

$$\langle (\Delta_\perp r)^2(t)\rangle = \langle (\Delta r)^2(t)\rangle - \langle (\Delta_\parallel r)^2(t)\rangle, \tag{5}$$

where $\mathbf{R}_E(t = 0)$ is the end-to-end vector of the nanorod at time $t = 0$. $A(t)$ is defined as follows:

$$A(t) \equiv 3 \frac{\langle (\Delta_\parallel r)^2(t)\rangle}{\langle (\Delta r)^2(t)\rangle} - 1. \tag{6}$$

$A(t)$ allows us to quantify how much the nanorod translate parallel to the end-to-end vector of the nanorod. When the translational diffusion is isotropic, $A(t) = 0$, whereas $A(t) = 2$ if the nanorod would translate only in the direction parallel to $\mathbf{R}_E(t = 0)$. The translational relaxation time (τ_T) of the nanorod is also obtained by using the relation, $\langle (\Delta r)^2(t)\rangle (t = \tau_T) = \langle R_g^2\rangle$. Here, $\langle R_g^2\rangle$ is the mean-square radius of gyration of the nanorod.

III. RESULTS AND DISCUSSION

The persistence length (l_p) of the nanorod increases sharply with the force constant K_b of the bending potential $U_b(\theta)$. We estimate l_p using the relation $l_p = \sigma/(1 + \langle \cos\theta\rangle)$, where θ is the angle between two consecutive chemical bonds of the nanorod [49]. As depicted in Fig. 3(a), l_p increases from $l_p = 1.65$ for $K_b = 0$ to $l_p = 41.19$ for $K_b = 20$ in polymer melts of $N = 32$. Because $l_p \approx 20$ for $K_b \approx 10$ and the contour length of the nanorod is only 20 ($N_{\rm rod} = 20$), the nanorod should

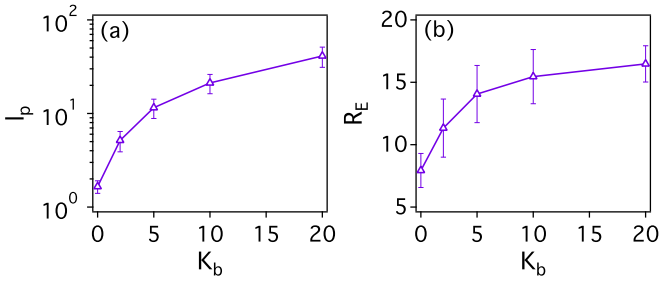

FIG. 3. (Color online) Simulation results for (a) the persistence length (l_p) and (b) the mean-square end-to-end distance (R_E) of a single nanorod as a function of K_b. In this case, $N = 32$ and $\rho = 0.8$.

be quite stiff when $K_b > 10$. The length of the nanorod is also characterized by the root mean-square end-to-end distance (R_E) as follows [50]:

$$R_E = \sqrt{\left\langle \left(\mathbf{r}_1 - \mathbf{r}_{N_{\rm rod}}\right)^2 \right\rangle}, \tag{7}$$

where $\mathbf{r}_1$ and $\mathbf{r}_{N_{\rm rod}}$ are the position vectors of the first and the last beads of the nanorod. When $K_b = 0$, R_E is only 7.9. On the other hand, when $K_b > 10$, R_E is much larger: around $R_E \approx 16.5$.

The site-site intermolecular correlation function [$g_{NP}(r)$] between the nanorod and polymers is insensitive to the degree of polymerization (N) of the polymers [Fig. 4(a)]. This is attributed to the relatively high number density ($\rho = 0.8$) of the polymer melts. Regardless of N, the first shell of monomers around beads of the nanorod forms for $r \leqslant 1.5\sigma$. On the other hand, the site-site intermolecular correlation function [$g_{PP}(r)$] between polymers depend on the values of N, especially for the first and second peak heights. Those peak heights decrease with an increase in N because two monomers of different chains are less likely to contact each other for longer polymers.

The translational and rotational diffusion of the nanorod slow down as N increases. The slow-down of the diffusion coefficient may be attributed mainly to the increase in viscosity (η) of polymer melts with the degree of polymerization N. Figure 5 depicts both $\langle (\Delta r)^2(t)\rangle$ and $U(t)$ of the nanorod for $K_b = 20$ and various values of N. The translational diffusion of the nanorod reaches the Fickian diffusion regime within our simulation times for all values of N, i.e., $\langle (\Delta r)^2(t)\rangle \sim t^1$. $\langle (\Delta r)^2(t)\rangle$ decreases with an increase in N but does not decrease much from $N = 32$ to $N = 64$. On the other hand, $U(t)$ decays more slowly as N increases from 1 to 64.

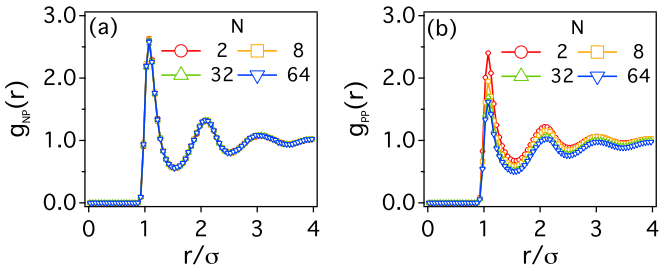

FIG. 4. (Color online) (a) The site-site intermolecular correlation functions [$g_{NP}(r)$] between the nanorod and polymers and (b) site-site intermolecular correlation functions [$g_{PP}(r)$] between polymers.

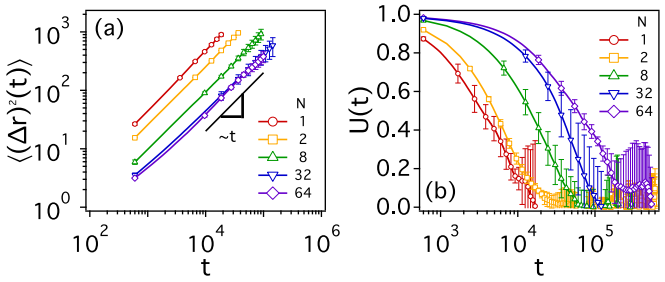

FIG. 5. (Color online) (a) $\langle(\Delta r)^2(t)\rangle$ and (b) $U(t)$ of the nanorod in polymer melts for $K_b = 20$ and different values of N.

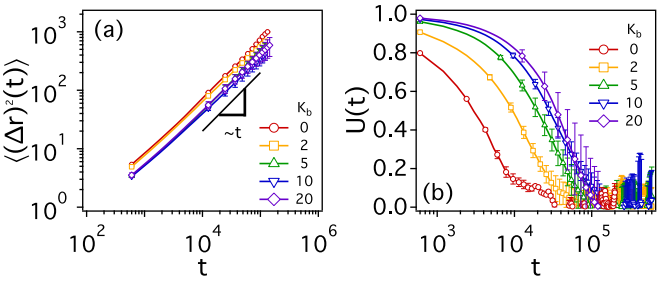

FIG. 7. (Color online) (a) $\langle(\Delta r)^2(t)\rangle$ and (b) $U(t)$ of the nanorod in polymer melts for $N = 32$ and different values of K_b.

Note that the abscissa has a logarithmic scale in Fig. 5(b). Figures 6(a) and 6(b) depict the translational diffusion coefficient (D_T) and the translational and rotational relaxation times (τ_T and τ_R). D_T decreases with an increase in N. When $N \leqslant 32$, D_T decreases with N slightly more slowly than expected by the Stokes-Einstein relation, i.e., $D_T \sim N^{-0.71}$. But in the case of $N = 64$ the translational diffusion is much faster than expected by the Stokes-Einstein relation. Such a change in D_T is reflected in the translational relaxation time τ_T [Fig. 6(b)]. On the other hand, τ_R increases with N more significantly. τ_R increases by a factor of 17.7 from $N = 1$ to 64 while τ_T increases only by a factor of 12.1. Comparing the relative translational and rotational relaxation times, the translational diffusion slows down less significantly than the rotational diffusion, thus decoupling the translational and rotational diffusion of the nanorod even in unentangled polymer melts. Such decoupling might be attributed to the anisotropic nature of the translational motion of the nanorod. As will be discussed below, the translational diffusion of the nanorod becomes significantly anisotropic, especially in polymer melts of $N = 64$. This implies that the nanorod would experience different drag forces depending on whether the nanorod translates parallel or perpendicular to the end-to-end vector of the nanorod. The structural and dynamic anisotropies intrinsic in the nanorod may complicate its translational diffusion behavior.

For a given polymer length (N), the translational diffusion of the nanorod is relatively less dependent on its flexibility than the rotational diffusion. Figure 7 depicts $\langle(\Delta r)^2(t)\rangle$ and $U(t)$ for $N = 32$ and various values of K_b. The rotational relaxation of the nanorod slows down with an increase in K_b.

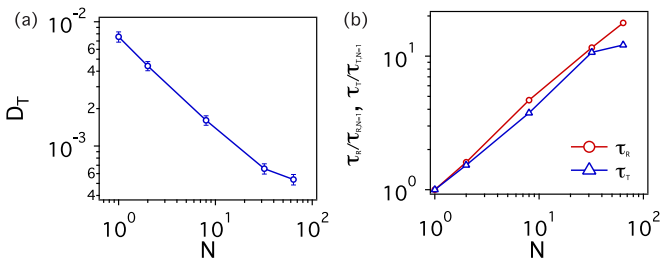

FIG. 6. (Color online) (a) The translational diffusion coefficient D_T and (b) relative relaxation times ($\tau_T/\tau_{T,N=1}$ and $\tau_R/\tau_{R,N=1}$) of the nanorod in polymer melts for $K_b = 20$ and different values of N. $\tau_{T,N=1}$ and $\tau_{R,N=1}$ are the translational and rotational relaxation times of the nanorod for $N = 1$.

The rotational diffusion slows down more with K_b than the translational diffusion because more energy would be required for a stiffer (therefore longer and more anisotropic) nanorod to change its conformation and rotate in dense polymer melts.

Longer polymers are more likely to wind the nanorod. In our simulations, polymers of $N \leqslant 32$ hardly wind the nanorod. Only the longest polymers of $N = 64$ are capable of winding the nanorod to some extent. Figure 8 depicts the probability distribution function $P(W)$ for different values of K_b and N. As shown in Fig. 8(a), for a given value of $K_b = 20$, only when $N = 64$ are polymers able to wind the nanorod more than halfway around the nanorod perimeter, i.e., $W \geqslant 0.5$. When $N < 64$, $P(W)$ hardly changes with the nanorod stiffness (K_b). When $N = 64$, a more flexible nanorod is wrapped more efficiently by polymers. But the difference in $P(W)$'s for different K_b is within our simulation errors.

The winding number (W) and its probability distribution [$P(W)$] provide information on how a single neighbor polymer winds the nanorod. Because there are many neighbor polymers around the nanorod in dense polymer melts, a few neighbor polymers, at least in principle, may wind the nanorod simultaneously. When investigating the nanorod dynamics, therefore, it would be necessary to consider the overall effects of multiple neighbor polymers that wind the nanorod at the same time. We investigate the total winding number (T) and the effective winding number (S). T is defined as the sum of all winding numbers W's for all neighbor polymers at a given time (or a given configuration). S is the sum of values of only W's that are larger than 0.5. Therefore, when estimating S, we count only polymers that wind the nanorod effectively with $W \geqslant 0.5$.

As depicted in Fig. 9, $P(T)$'s for $N = 8, 32$, and 64 are quite similar to each other, indicating that the overall sum of W's is not sensitive to N. This would be partially attributed to the fact

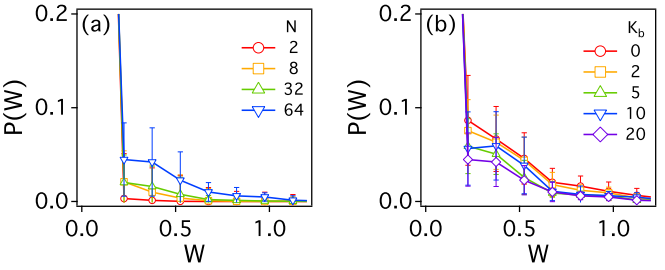

FIG. 8. (Color online) The probability distribution functions [$P(W)$] of the winding number W for (a) $K_b = 20$ and (b) $N = 64$.

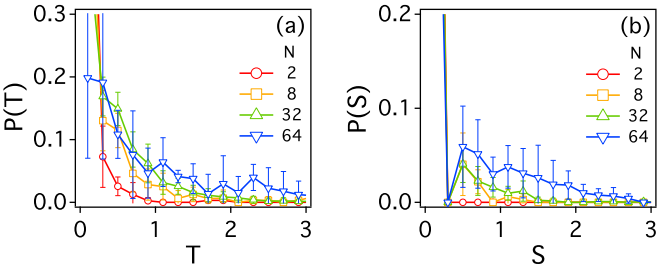

FIG. 9. (Color online) (a) The probability distribution functions $P(T)$ of the total winding number T and (b) the probability distribution functions $P(S)$ of the effective winding number S. $K_b = 20$ and N ranges from 2 to 64.

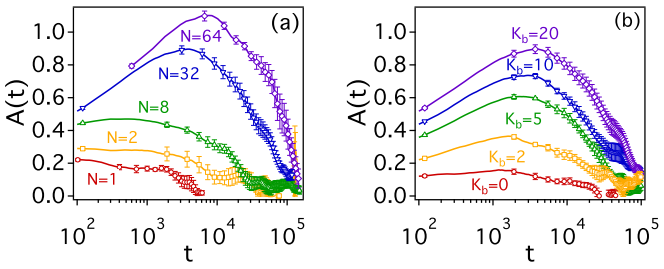

FIG. 11. (Color online) $A(t)$ of the nanorod for (a) $K_b = 20$ and different values of N and (b) $N = 32$ and different values of K_b.

that $g_{NP}(r)$'s are insensitive to N and there are similar numbers of neighbor monomers per nanorod bead regardless of N. In the mean time, $P(S)$ for $N = 64$ shows a pronounced increase for $S \geqslant 0.5$ compared to other values of N. This suggests that in the case of $N = 64$ there are several polymers that wind the nanorod effectively with $W \geqslant 0.5$. The values of S reach up to 5.1 for $N = 64$. Considering that W reaches usually up to 0.6 for $N = 64$ [in the case of $K_b = 20$, as in Fig. 8(b)], there may be some instances when up to six neighbor polymers wind the nanorod effectively at the same time. For example, as shown in Fig. 10, the nanorod (yellow) is wrapped by six neighbor polymers with $W \geqslant 0.5$. Winding numbers for red, orange, green, pink, purple, and ice-blue neighbor polymers are 0.93, 0.56, 0.94, 0.71, 0.81, and 0.56, respectively, thus $S = 4.51$ in this particular case. This clearly shows that, even though large values of S are still scarce, the anisotropic nanorod may be wrapped by many neighbor polymers simultaneously, thus making the dynamics of the nanorod a complicated many-body problem.

The nanorod tends to translate in an anisotropic fashion as either the degree of polymerization N increases or the nanorod becomes stiffer (with larger K_b). Figure 11(a) depicts

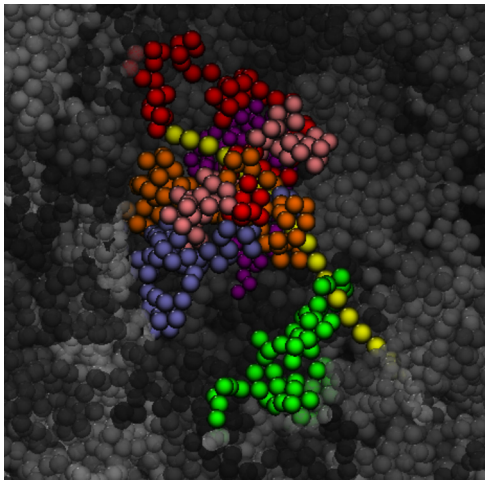

FIG. 10. (Color online) A simulation snapshot for a single nanorod (yellow) in polymers melts of $N = 64$. Red, orange, green, pink, purple, and ice-blue neighbor polymers wind the nanorod at the same time with winding numbers $W = 0.93$, 0.56, 0.94, 0.71, 0.81, and 0.56, respectively. All other polymers are colored in grey.

$A(t)$ for $K_b = 20$. A larger value of $A(t)$ indicates that the nanorod undergoes translational motion more in the direction of an end-to-end vector. Because multiple polymers may wrap the nanorod effectively when $N \geqslant 64$, $A(t)$ increases significantly for long chains with $N \geqslant 64$. For $K_b = 20$ and $N = 64$, $A(t)$ shows a maximum at around $t = t_{\max} \approx 10^4$. Because $t_{\max} < \tau_T (\approx 1.8 \times 10^4) < \tau_R (\approx 8 \times 10^4)$, the anisotropy in translational motion of the nanorod is maximized before the nanorod translates about its own size (R_g) and well before the rotational relaxation decays completely. However, when $t \approx 10^5 > \tau_R > \tau_T$, $A(t)$ decreases quickly, implying that the anisotropy in translational motion goes away at such time scales. As depicted in Fig. 11(b), the anisotropy in the translational motion increases quickly with the nanorod stiffness, or K_b. This suggests that the anisotropic translation dominates when a stiffer nanorod is wrapped by long polymers.

In order to investigate whether the anisotropic translational diffusion of the nanorod would relate to polymers winding the nanorod, we estimate the conformational correlation between neighbor polymers and the nanorod. We calculate the orientational correlation coefficient (S_2) between the end-to-end vectors of the nanorod and the local segment of a polymer. We define N_{seg} consecutive monomers of the single polymer as the local segment of size N_{seg}. All N_{seg} monomers are connected via $N_{\text{seg}} - 1$ chemical bonds. There are, therefore, $N - N_{\text{seg}} + 1$ local segments of size N_{seg} for each polymer. $S_2 \equiv \frac{1}{2}(3\langle \cos^2(\theta) - 1 \rangle)$, where θ is the angle between two end-to-end vectors of the nanorod and the local segment. S_2 is averaged over all neighbor polymers and configurations. When the orientation of the local segment is parallel, perpendicular, and uncorrelated to that of the nanorod, $S_2 = 1$, -0.5, and 0, respectively. In Fig. 12(a), we plot S_2 as a function of the shortest distance ($r_{\min}$) between the local segment and the nanorod. For large values of $r_{\min}$, $S_2 = 0$ because there is no orientational correlation between the nanorod and the local segment. As $r_{\min}$ decreases, on the other hand, S_2 becomes negative, implying that local segments of polymers around the nanorod are likely to align perpendicular to the nanorod. For smaller local segments, the decrease in S_2 for small values of $r_{\min}$ is even more pronounced. Such a negative value of S_2 arises because the local segment winds the nanorod, which is consistent with simulation snapshots (Fig. 10). Because the local segment aligns perpendicular to the nanorod and winds the nanorod, the translational motion of the nanorod is restricted in the direction perpendicular to its end-to-end vector. In other words, while local segments of polymers wind the nanorod, the nanorod can translate only parallel

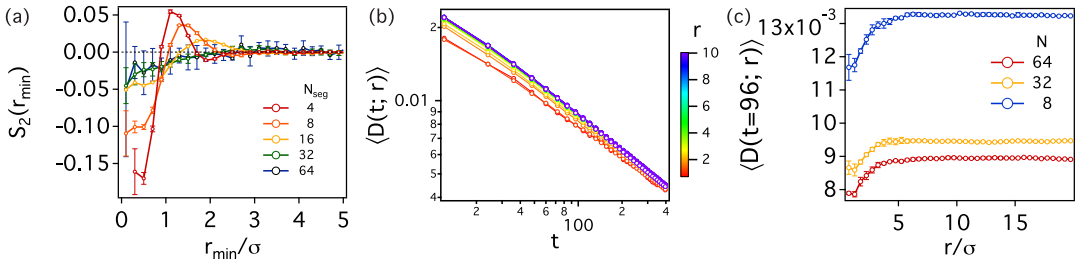

FIG. 12. (Color online) (a) The orientational correlation coefficient (S_2) between two end-to-end vectors of both the nanorod and the local segment of polymers as a function of the shortest distance ($r_{\rm min}$) between the local segment and the nanorod. (b) The time-dependent diffusion coefficient $\langle D(t;r)\rangle$ as a function of time t for different initial shortest distance r between the monomer and the nanorod for $N = 64$ and $K_b = 20$. (c) $\langle D(t;r)\rangle$ of monomers during time $t = 96$ as a function of the initial shortest distance r.

to its end-to-end vector, thus making the nanorod diffusion anisotropic at certain time scales. Considering that multiple polymers of $N \geqslant 64$ may wind the nanorod at the same time (Fig. 10), the nanorod diffusion should be restricted more significantly in the perpendicular direction for longer polymers and the anisotropy in the nanorod diffusion should be more pronounced for the nanorod in longer polymer melts.

We also investigate the dynamics of monomers near the nanorod by calculating the time-dependent diffusion coefficient $\langle D(t;r)\rangle \equiv \langle(\Delta r)^2(t;r)\rangle$, where $\Delta r(t;r)$ is the displacement vector of a monomer during time t, and the shortest distance the monomer and the nanorod is r initially [51,52]. Figure 12(b) depicts $\langle D(t;r)\rangle$ as functions of the duration t for different values of the shortest distance r between a monomer and the nanorod. $\langle D(t;r)\rangle$ is smaller for smaller values of r, implying that the monomers at the interface between the nanorod and polymers would be less mobile than monomers far away from the nanorod. As t increases, the correlation between the nanorod and polymers becomes less significant and $\langle D(t;r)\rangle$ also becomes less sensitive to the values of r. We also plot $\langle D(t;r)\rangle$ as a function of r for a given value of $t = 96$ [Fig. 12(c)]. Not surprisingly, as N increases from 8 to 64, the mobility decreases for all ranges of r. This may be attributed to the fact that the longer polymer diffusion becomes significantly slower. Figure 12(c) shows clearly that monomers become less mobile as monomers approach the nanorod. Such a slow-down of monomers at the interface may result from both (1) the attractive interaction between the nanorod and monomers and (2) the winding of monomers around the nanorod. As discussed above, there is a stronger correlation between the nanorod orientation and the local segment, which also might affect the slow-down of monomers at the interface.

IV. SUMMARY AND CONCLUSIONS

The dynamics of a single nanorod in polymer melts is investigated by performing molecular dynamics simulations and investigating how much polymers may wind the nanorod. When N increases from 1 to 64, τ_T and τ_R increase by factors of 10 and 17.7, respectively. This shows that the rotational motion of the nanorod is hindered more than the translational motion. However, the translational diffusion becomes anisotropic at time scales shorter than τ_T. The translational anisotropy is maximized for the stiffest nanorod and the longest polymers. At time scales longer than τ_R, the anisotropy of the translational motion vanishes. Note, however, that the translational diffusion enters a Fickian regime even when the translational diffusion is anisotropic, i.e., $\langle(\Delta r)^2(t)\rangle \sim t^1$. For example, in the case of $(N, K_b) = (64, 20)$, the translational diffusion of the nanorod becomes the most anisotropic at $t \approx 10^4$ [Fig. 11(a)], $\langle(\Delta r)^2(t)\rangle \sim t^1$ at $t \approx 10^4$ [Fig. 7(a)].

Our simulations are performed only for relatively short polymers and a nanorod. As N increases beyond a certain value, polymers begin to entangle one another, which should affect the nanorod dynamics. It is well known that the translational diffusion of a nanoparticle changes qualitatively depending on the polymer correlation length (or the entanglement mesh size). Therefore, investigating the translational and rotational dynamics of the nanorod in entangled polymer melts is going to be a important topic in future studies.

ACKNOWLEDGMENTS

We acknowledge financial support from the Ministry of Education, Science, and Technology, to the project EDISON (Education-Research Integration through Simulation on the Net, Grant No. 2012M3C1A6035363). This research was supported by the Advanced Research Center for Nuclear Excellence, funded by MEST, Korea. This research was also supported by the Basic Science Research Program through the National Research Foundation of Korea (NRF), funded by the Ministry of Education, Science and Technology (NRF-2013R1A1A2009972).

M.J.K. and H.W.C. contributed equally to this work.

[1] R. C. Ferrier, H.-S. Lee, M. J. A. Hore, M. Caporizzo, D. M. Eckmann, and R. J. Composto, Langmuir **30**, 1906 (2014).

[2] V. Pryamitsyn and V. Ganesan, Macromolecules **39**, 844 (2006).

[3] F. Ko, Y. Gogotsi, A. Ali, N. Naguib, H. Ye, G. Yang, C. Li, and P. Willis, Adv. Mater. **15**, 1161 (2003).

[4] S. Nam, H. W. Cho, T. Kim, D. Kim, B. J. Sung, S. Lim, and H. Kim, Appl. Phys. Lett. **99**, 043104 (2011).

[5] S. B. Kharchenko, J. F. Douglas, J. Obrzut, E. A. Grulke, and K. B. Migler, Nat. Mater. **3**, 564 (2004).

[6] A. Balazs, T. T. Emrick, and T. P. Russell, Science **314**, 1107 (2006).

[7] S. Nam, H. W. Cho, S. Lim, D. Kim, H. Kim, and B. J. Sung, ACS Nano **7**, 851 (2013).
[8] N. Jouault, F. Dalmas, F. Boué, and J. Jestin, Polymer **53**, 761 (2012).
[9] D. Wang, M. J. A. Hore, X. Ye, C. Zheng, C. B. Murray, and R. J. Composto, Soft Matter **10**, 3404 (2014).
[10] M. E. Mackay, A. Tuteja, P. M. Duxbury, C. J. Hawker, B. Van Horn, Z. Guan, G. Chen, and R. S. Krishnan, Science **311**, 1740 (2006).
[11] M. J. A. Hore and R. J. Composto, Macromolecules **47**, 875 (2014).
[12] M. J. A. Hore and R. J. Composto, Curr. Opin. Chem. Eng. **2**, 95 (2013).
[13] Y. Gao, J. Liu, J. Shen, L. Zhang, and D. Cao, Polymer **55**, 1273 (2014).
[14] B. J. Blaiszik, S. L. B. Kramer, S. C. Olugebefola, J. S. Moore, N. R. Sottos, and S. R. White, Annu. Rev. Mater. Res. **40**, 179 (2010).
[15] F. Du, R. C. Scogna, W. Zhou, S. Brand, J. E. Fischer, and K. I. Winey, Macromolecules **37**, 9048 (2004).
[16] V. Ganesan, V. Pryamitsyn, M. Surve, and B. Narayanan, J. Chem. Phys. **124**, 221102 (2006).
[17] J. T. Kalathi, U. Yamamoto, K. S. Schweizer, G. S. Grest, and S. K. Kumar, Phys. Rev. Lett. **112**, 108301 (2014).
[18] J. Liu, D. Cao, and L. Zhang, J. Phys. Chem. C **112**, 6653 (2008).
[19] S. A. Egorov, J. Chem. Phys. **134**, 084903 (2011).
[20] D. M. Heyes, M. J. Nuevo, and J. J. Morales, J. Chem. Soc., Faraday Trans. **94**, 1625 (1998).
[21] A. Tuteja, M. E. Mackay, S. Narayanan, S. Asokan, and M. S. Wong, Nano Lett. **7**, 1276 (2007).
[22] J. T. Kalathi, G. S. Grest, and S. K. Kumar, Phys. Rev. Lett. **109**, 198301 (2012).
[23] C. D. Chapman, K. Lee, D. Henze, D. E. Smith, and R. M. Robertson-Anderson, Macromolecules **47**, 1181 (2014).
[24] C. A. Grabowski and A. Mukhopadhyay, Macromolecules **47**, 7238 (2014).
[25] U. Yamamoto and K. S. Schweizer, J. Chem. Phys. **135**, 224902 (2011).
[26] C. A. Grabowski, B. Adhikary, and A. Mukhopadhyay, Appl. Phys. Lett. **94**, 021903 (2009).
[27] B.-Y. Cao and R.-Y. Dong, J. Chem. Phys. **140**, 034703 (2014).
[28] H. Maeda and Y. Maeda, Nano Lett. **7**, 3329 (2007).
[29] P. Cassagnau, Polymer **54**, 4762 (2013).
[30] B. Senyuk, D. Glugla, and I. I. Smalyukh, Phys. Rev. E **88**, 062507 (2013).
[31] D.-H. Xu, Z.-G. Wang, and J. F. Douglas, Macromolecules **41**, 815 (2008).
[32] B. Wang, J. Guan, S. M. Anthony, S. C. Bae, K. S. Schweizer, and S. Granick, Phys. Rev. Lett. **104**, 118301 (2010).
[33] M. P. Lettinga, E. Barry, and Z. Dogic, Europhys. Lett. **71**, 692 (2005).
[34] T. Zhao and X. Wang, Polymer **54**, 5241 (2013).
[35] J. Choi, M. J. A. Hore, J. S. Meth, N. Clarke, K. I. Winey, and R. J. Composto, ACS Macro Lett. **2**, 485 (2013).
[36] U. Yamamoto and K. S. Schweizer, ACS Macro Lett. **2**, 955 (2013).
[37] S. Gam, J. S. Meth, S. G. Zane, C. Chi, B. A. Wood, M. E. Seitz, K. I. Winey, N. Clarke, and R. J. Composto, Macromolecules **44**, 3494 (2011).
[38] C.-C. Lin, S. Gam, J. S. Meth, N. Clarke, K. I. Winey, and R. J. Composto, Macromolecules **46**, 4502 (2013).
[39] S. Gam, J. S. Meth, S. G. Zane, C. Chi, B. A. Wood, and K. I. Winey, Soft Matter **8**, 6512 (2012).
[40] J. S. Meth, S. Gam, J. Choi, C.-C. Lin, R. J. Composto, and K. I. Winey, J. Phys. Chem. B **117**, 15675 (2013).
[41] M. Mu, R. J. Composto, N. Clarke, and K. I. Winey, Macromolecules **42**, 8365 (2009).
[42] M. Mu, N. Clarke, R. J. Composto, and K. I. Winey, Macromolecules **42**, 7091 (2009).
[43] A. Karatrantos, R. J. Composto, K. I. Winey, M. Kröger, and N. Clarke, Macromolecules **45**, 7274 (2012).
[44] M. Mu, M. E. Seitz, N. Clarke, R. J. Composto, and K. I. Winey, Macromolecules **44**, 191 (2011).
[45] D. G. Richardson and C. F. Abrams, Macromolecules **39**, 2330 (2006).
[46] G. N. Toepperwein, N. C. Karayiannis, R. A. Riggleman, M. Kröger, and J. J. de Pablo, Macromolecules **44**, 1034 (2011).
[47] A. Karatrantos, N. Clarke, R. J. Composto, and K. I. Winey, Soft Matter **9**, 3877 (2013).
[48] J. Hansen and I. McDonald, *Theory of Simple Liquids* (Academic Press, London, 2006).
[49] H. T. Jung, B. J. Sung, and A. Yethiraj, J. Polym. Sci. Part B: Polym. Phys. **49**, 818 (2011).
[50] M. Rubinstein and R. H. Colby, *Polymer Physics* (Oxford University Press, New York, 2007).
[51] V. A. Harmandaris, K. C. Daoulas, and V. G. Mavrantzas, Macromolecules **38**, 5796 (2005).
[52] A. N. Rissanou, A. J. Power, and V. Harmandaris, Polymer **7**, 390 (2015).